Published in final edited form as:
Arch Biochem Biophys. 2013 January 1; 529(1): 45–54. doi:10.1016/j.abb.2012.10.012.

Peroxynitrite formation in nitric oxide-exposed submitochondrial particles: Detection, oxidative damage and catalytic removal by Mn-porphyrins

Valeria Valez[1], **Adriana Cassina**[1,2], **Ines Batinic-Haberle**[3], **Balaraman Kalyanaraman**[4], **Gerardo Ferrer-Sueta**[1,5], and **Rafael Radi**[1,2,*]

[1]Center for Free Radical and Biomedical Research, Universidad de la República, Avda. General Flores 2125, Montevideo 11800, Uruguay

[2]Departamento de Bioquímica, Facultad de Medicina, Universidad de la República, Avda. General Flores 2125, Montevideo 11800, Uruguay

[3]Department of Radiation Oncology, Duke University Medical Center, Durham, North Carolina

[4]Biophysics Research Institute and Free Radical Research Center, Medical College of Wisconsin, Milwaukee, Wisconsin, United States of America

[5]Laboratorio de Fisicoquímica Biológica, Facultad de Ciencias, Universidad de la República, Montevideo 11400, Uruguay

Abstract

Peroxynitrite ($ONOO^-$) formation in mitochondria may be favored due to the constant supply of superoxide radical ($O_2^{\bullet -}$) by the electron transport chain plus the facile diffusion of nitric oxide ($^\bullet NO$) to this organelle. Herein, a model system of submitochondrial particles (SMP) in the presence of succinate plus the respiratory inhibitor antimycin A (to increase $O_2^{\bullet -}$ rates) and the $^\bullet NO$-donor NOC-7 was studied to directly establish and quantitate peroxynitrite by a multiplicity of methods including chemiluminescence, fluorescence and immunochemical analysis. While all the tested probes revealed peroxynitrite at near stoichiometric levels with respect to its precursor radicals, coumarin boronic acid (a probe that directly reacts with peroxynitrite) had the more straightforward oxidation profile from $O_2^{\bullet -}$-forming SMP as a function of the $^\bullet NO$ flux. Interestingly, immunospintrapping studies verified protein radical generation in SMP by peroxynitrite. Substrate-supplemented SMP also reduced Mn(III)porphyrins (MnP) to Mn(II)P under physiologically-relevant oxygen levels (3–30 μM); then, Mn(II)P were capable to reduce peroxynitrite and protect SMP from the inhibition of complex I-dependent oxygen consumption and protein radical formation and nitration of membranes. The data directly support the formation of peroxynitrite in mitochondria and demonstrate that MnP can undergo a catalytic redox cycle to neutralize peroxynitrite-dependent mitochondrial oxidative damage.

*Correspondence should be addressed to Rafael Radi, MD, PhD, Departamento de Bioquímica, Facultad de Medicina, Universidad de la República, Av. General Flores 2125, 11800 Montevideo, Uruguay. Tel: (+5982)924-95-61. Fax: (+5982)924-95-63; rradi@fmed.edu.uy.

Keywords

Mitochondrial oxidative stress; submitochondrial particles; manganese porphyrin; free radicals; superoxide radical-antioxidants

INTRODUCTION

Peroxynitrite anion is formed by the diffusion-controlled reaction of superoxide ($O_2^{\bullet -}$) and nitric oxide ($^{\bullet}NO$) radicals (k *ca.* 1×10^{10} M^{-1} s^{-1} [1]); together with its conjugated acid (ONOOH) (p*Ka*= 6.8), it represents a potent oxidizing and nitrating species formed *in vivo* [2]. Peroxynitrite is typically formed in the vicinity of $O_2^{\bullet -}$-generation sites, and therefore mitochondria were early recognized to constitute major intracellular sources [3]. Indeed, the formation and actions of peroxynitrite in mitochondria are favored because of the special features of this organelle in cellular redox metabolism and bioenergetics (reviewed in [4,5]). First, the electron transport chain (*e.g.* at complexes I and III) represents a major intracellular source of $O_2^{\bullet -}$, especially during alterations in mitochondrial function and homeostasis; then, the arrival of $^{\bullet}NO$ from vicinal compartments by diffusion [6] or its generation inside mitochondria [7] facilitates the combination reaction with inner membrane-derived $O_2^{\bullet -}$ to yield peroxynitrite *in situ*. While mitochondrial superoxide dismutase (MnSOD) minimizes peroxynitrite formation and peroxiredoxins 3 and 5 promote its decomposition [1], even under basal physiological conditions mitochondria contain the largest yield of nitrated proteins, underscoring their contribution as key intracellular sources of peroxynitrite and nitrating species [8].

Peroxynitrite interacts with mitochondrial protein and lipids and, at elevated levels, causes oxidative damage [3,5]. In particular, peroxynitrite interacts with the inner mitochondrial membrane components, producing a strong inhibition of complex I (NADH dehydrogenase)- and complex II (succinate dehydrogenase)-dependent oxygen consumption [6,9]. Complex I inactivation is associated with thiol oxidation and S-nitrosation and nitration of specific tyrosines residues [10,11]. Complex II inactivation may also involve the oxidation of the critical thiol in Cys^{252} of subunit A [12]. Peroxynitrite also affects the mitochondrial ATP synthase [6,9], presumably *via* oxidative modification of critical tyrosine residues (Tyr^{368} of beta subunit of F_1) and thiols that are involved in the F_1F_0 interaction [13]. Overall, the interactions of peroxynitrite with respiratory chain components result in altered electron transport fluxes, inhibition of oxygen consumption and ATP synthesis and increased mitochondrial $O_2^{\bullet -}$ formation rates [9,12].

Studies have evidenced the formation of peroxynitrite in mitochondria through its effects exerted on proteins and lipids [4,14]. Alternatively, other studies have indirectly revealed the production of peroxynitrite in mitochondria either by following the consumption of exogenously added $^{\bullet}NO$ [15] or through the protective action of MnSOD overpression [16] and compounds such as manganese porphyrins (MnP), known to react and reduce peroxynitrite [17], on $^{\bullet}NO$-mediated toxicity. Thus, while there are scattered and indirect evidences supporting the formation of peroxynitrite in mitochondria, a more explicit, robust and quantitative analysis is lacking. First, fluorescence and chemiluminescence probes previously utilized to detect peroxynitrite and its derived radicals (*e.g.*dihydrorhodamine 123; DHR, 2,7-dichlorodihydrofluorescein diacetate; DCDHF or luminol) can be useful but can easily lead to ambiguous or even erroneous results if used in isolation or without appropriate controls [18]. More recently, boronate-based compounds, including the fluorogenic coumarin-7-boronic acid, have been developed and used as rapid and quantitative probes for peroxynitrite detection in biological systems [19]: thus, its application in mitochondria represents a prime opportunity. Second, while oxidative

modifications of mitochondrial proteins by peroxynitrite have been followed immunochemically by the detection of nitrotyrosine [4], the recent development of immunospintrapping to detect protein-derived radicals *in vitro* [20] and even *in vivo* [21], provides a further chance to evaluate mitochondrial protein modifications by peroxynitrite with even higher sensitivity. Herein, we have used and validated a series of methods to establish the formation of peroxynitrite in a model system consisting of submitochondrial particles (SMP) exposed to •NO. The selected model system provides a proof –of –concept to assess and quantitate peroxynitrite-dependent processes in mitochondria; this simplified mitochondrial structure has the advantage to include a functional electron transport chain, also responsible of $O_2^{\bullet -}$ -formation, while lacking enzymatic antioxidant systems, and has been previously used to assess effects of •NO on mitochondrial oxygen consumption [15]. Thus, in the SMP system studied herein, yields and some effects of peroxynitrite could be measured in a more amenable and convincing manner.

Then, under conditions of peroxynitrite generation by SMP, we evaluated the antioxidant potential of MnP as peroxynitrite reducing compounds [22,23]. We have recently found that complex I and II can reduce MnP(III) to Mn(II)P, which can, in turn, reduce peroxynitrite to nitrite NO_2^- and protect mitochondrial components [23]. However, in the previous work MnP reduction by the respiratory chain complexes was tested under very low oxygen tensions only. Thus, a remaining question is whether at the range of oxygen levels that exist in most mitochondria under physiological conditions (*e.g.* 3–30 μM [24]), the Mn(III)P can compete well and sufficiently fast for the uptake of electrons from the electron transport chain resulting in its reduction to Mn(II)P and subsequent protection from peroxynitrite-dependent damage. To address this issue we have followed the reduction of two different MnP differing in hydrophobicity and redox potential by SMP as a function of oxygen levels; in addition, we examined the protective effect of MnP on the activity of respiratory chain complexes and on mitochondrial protein oxidation and nitration during the endogenous generation or exogenous challenge with peroxynitrite. The data mechanistically support a central role of mitochondria as key sources of peroxynitrite and demonstrate that catalytic redox cycles of MnP in mitochondria attenuate peroxynitrite-dependent damage.

EXPERIMENTAL PROCEDURES

Reagents

All reagents were obtained from standard commercial sources and used as received unless otherwise indicated. The chemiluminescence probes luminol and coelenterazine were obtained from Sigma and Calbiochem, respectively. Dihydrorhodamine-123 (DHR) was obtained from Molecular Probes-Invitrogen (Eugene, OR). NOC-7 and 5,5-dimethyl-1-pyrroline-*N*-oxide (DMPO) were from Dojindo Laboratories. Antibodies against DMPO–protein adducts were kindly provided by Dr. Ronald P. Mason of the National Institute of Environmental Health Sciences, Research Triangle Park, NC [25]. The MnP used were MnTE-2-PyP^5 Mn(III) *meso*-tetrakis (*N*-ethyl) pyridinium-2-yl)porphyrin(5+) and MnTnHex-2-PyP^{5+}, Mn(III) *meso*-tetrakis (N-n-hexyl) pyridinium-3-yl)porphyrin(5+) [26]. Coumarin -7- boronic acid (CBA) was synthesized as previously [19]. Acetylated cytochrome c was prepared as previously [27].

Mitochondria and submitochondrial particles purification

Rat heart mitochondria were isolated and purified by differential centrifugation as described previously [6]. Briefly, rats were anesthetized, and the heart was removed and washed extensively, minced, and homogenized with a small tissue grinder. Tissue fragments were disrupted using a Potter-Elvehjem homogenizer in a solution containing sucrose (0.3 M), MOPS (5 mM), potassium phosphate (5 mM), EGTA (1 mM), and 0.1% bovine serum

albumin (BSA) (homogenization buffer). The homogenate was then centrifuged at 1500 × *g*, and mitochondria were isolated from the supernatant by centrifugation at 13,000 × *g*. Mitochondrial pellets were resuspended in minimal volume of homogenization buffer. SMP were obtained from bovine heart and characterized by published procedures [28].

Peroxynitrite synthesis and quantitation

Peroxynitrite was synthesized, quantitated and handled as described previously [29]. Peroxynitrite concentrations were determined spectrophotometrically at 302 nm (ε = 1670 M^{-1} cm^{-1}) [30]. The nitrite concentration in the preparations was typically lower than 20% with respect to peroxynitrite. Control of nitrite levels was critical for obtaining reproducible data as, if present in excess, it can react with $^{\bullet}OH$ and other oxidants and yield $^{\bullet}NO_2$ [30].

Nitric oxide preparation, quantitation and utilization

Nitric oxide stock solutions were prepared by gently bubbling $^{\bullet}NO$ gas for 10 min into a washing flask containing 5 M NaOH, which was trapped in a gas sampling tube containing deoxygenated deionized water. The nitric oxide concentration obtained was 1.5 mM, close to saturation levels at 25°C. Stock solution of NOC-7 (1 or 10 mM) from Alexis was prepared in 0.1 M NaOH. $^{\bullet}NO$ fluxes were quantitated following the oxidation of oxyhemoglobin to methemoglobin at 577 nm and 630 nm, according to [31] for 10 minutes (as an example, 1, 3, 6, 10, 25 and 50 μM correspond with linear fluxes for 5–8 minutes of 0.1, 0.3, 0.45, 0.7, 1.4, 2.4 μM min^{-1} at 37°C, respectively).

Chemiluminescencence measurements

Luminol (5-amino-2,3-dihydro-1,4-phthalazinedione) and coelenterazine (2- (4-hydroxybenzyl)-6-(4-hydroxyphenyl)-8-benzyl-3,7-dihydroimidazo[1,2-a]pyrazin-3-one)) were used as chemiluminescence probes; both compounds are used for detection of a variety of oxidants including peroxynitrite and oxygen radical species formed in biological systems (such as $O_2^{\bullet-}$ and $^{\bullet}OH$) [32,33] [34,35,36] and lead to the formation of excited species *via* free radical intermediates, which decay with the emission of light. Luminol (1 mM) stock solutions were prepared in water and adjusted to pH 8.0 with 1.0N NaOH. Coelenterazine was prepared in ethanol and its concentration was confirmed spectrophotometrically at 427 nm (ε =7400 $M^{-1}cm^{-1}$).

Chemiluminescence was monitored using a Thorn Emi photon counter equipped with an EMI Fact 50 MK III photomultiplier. The voltage in the photomultiplier was kept at 1500 V. The reactions were always carried out in glass tubes containing 3–5 mL of the samples, which were kept at 37°C by a temperature-controlled water bath. A magnetic stir bar was placed inside the sample tube to maintain continuous agitation. Data acquisition and analysis were performed with DQ software (DI-100 WINDATAQ, DATAQ Instruments, Inc., OH). Other experiments with luminol were performed in the LUMIstar Galaxy BMG Labtechnologies at 37°C with continuous agitation.

Measurement of superoxide radical formation by submitochondrial particles

Superoxide formation rates by SMP was quantitated by two independent methods, namely, the $O_2^{\bullet-}$- dependent reduction of acetylated cytochrome c (ε_{550} = 21 $mM^{-1}cm^{-1}$, [27]) and the fluorimetric detection of $O_2^{\bullet-}$-derived hydrogen peroxide by the horseradish peroxidase-catalyzed oxidation of Amplex Red (λ_{ex}= 563 nm, λ_{em}= 587 nm, [37]). Maximal $O_2^{\bullet-}$ formation rates were obtained by the supplementation of SMP with the combination of succinate (respiratory substrate) plus antimycin A (inhibitor), that triggers $O_2^{\bullet-}$-at mitochondrial complex III [38]. Calibrations of the different $O_2^{\bullet-}$-detecting systems were

performed using the xanthine/xanthine oxidase or glucose oxidase systems, as in previous works [33,39].

Fluorescent probes for peroxynitrite detection: dihydrorhodamine-123 and coumarin - 7 – boronic acid oxidation

DHR 123 oxidation to rhodamine was used to evaluate peroxynitrite production of SMP under different conditions (with succinate as substrate and antimycin A plus a $^{\bullet}$NO donor) [2,33]. Rhodamine (RH) is obtained after a two sequential one-electron oxidations of DHR 123 by peroxynitrite-derived radicals (*i.e.* with the intermediacy of semi-oxidized DHR-derived radical [40,41]; RH formation after exposure to the different experimental conditions was followed online in a fluorescence plate reader (Fluostar; BMG Lab technologies, Offenburg, Germany) with continuous orbital shaking, at 37°C for 20 min with λ_{ex} = 485 nm and λ_{em} = 520 nm. The slope represents the oxidation rate of DHR and was determined by the linear fit the first 3 – 5 minutes. Peroxynitrite formation by SMP was further evaluated by CBA. The fast direct reaction between CBA and peroxynitrite (k = 1.1 × 10^6 $M^{-1}s^{-1}$) yields the hydroxylated product, 7-hydroxycoumarin (COH) that can be followed at λ_{ex} = 330 nm and λ_{em} = 450 nm [19] in a fluorescence plate reader (Fluostar, BMG Lab Technologies, Offenburg, Germany) with continuous orbital shaking, at 37°C for 20 min, with filters at λ_{ex} = 320 nm and λ_{em} = 460 nm. The slope represents the oxidation rate of CBA and was determined by the linear fit of the first 3 – 5 minutes.

Immunochemical detection of protein nitrotyrosine and protein–spin trap adducts

Protein samples (30–40 μg) were separated on a 12% SDS-polyacrylamide gel and transferred to nitrocellulose membrane (GE Healthcare, Piscataway, NJ) overnight at 100 mA and 4°C. The immunochemical detection of protein 3-nitrotyrosine was carried out with a highly specific polyclonal anti-nitrotyrosine antibody developed in our laboratory as previously described [42]. For protein 3–nitrotyrosine immunodetection membranes were blocked 1 at room temperature (RT) in Tris-buffered saline (TBS) containing Tris pH 7.4 (25mM), NaCl (140 mM), and KCl (3 mM), supplemented with 0.6% vol/vol tween-20 and 5% wt/vol BSA. After that, membranes were incubated with the polyclonal rabbit anti-3-nitrotyrosine antibody at 1:2000 in the same blocking buffer 1 h at RT with gentle agitation. Membranes were washed 4 times for 5 minutes each in TBS plus 0.6% tween-20. Then, membranes were incubated with peroxidase-conjugated secondary antibody (Bio-Rad, Hercules, CA) diluted at 1:10000 in TBS, 0.3% tween-20, plus 0.1% BSA, for 1 h at RT. Membranes were washed 4 times as before. Membranes from western blot for protein 3-nitrotyrosine antibody were detected using the Immun-Star Chemiluminescence Kit (Bio-Rad). For DMPO immunospintrapping, membranes were blocked for 1 h in PBS, 5% milk at room temperature and slow agitation. Then washed 4 times for 5 minutes with PBS 0.2% tween-20 (washing buffer). After that 1 h incubation with primary anti-DMPO antibody at 1:5000 dilution in the same washing buffer at room temperature and slow agitation. After washing (4 times as before), the membrane was incubated with secondary antibody anti-Mouse IR Dye 800CW (LI-COR) at 1:20000 for 1 h in PBS plus 0.2 % tween-20 for 1 h at RT under slow agitation protected from light. Immuno reactive proteins were detected and quantified using the Odissey Infrared Imaging System.

Simultaneous measurement of oxygen levels and manganese porphyrin reduction by the electron transport chain

Mn(III)Porphyrin reduction by SMP was followed spectrophotometrically in a Cary 50 Tablet UV-visible spectrophotometer and oxygen levels were measured using a Clark-type electrode. A mixture consisting of 1 to 5 μM Mn(III)porphyrin, 0.1 – 0.5 mg protein/mL SMP or rat heart mitochondria, and either 2.5 mM succinate or 1 mM NADH in homogenization buffer or isotonic phosphate buffer (80 mM, potassium phosphate; 10 mM,

KCl; 40 mM, NaCl) pH 7.4, was incubated at 37°C and its time-dependent UV-Vis spectra was monitored from 350 to 600 nm or at 439 and 454 nm to follow the reduction process of MnP [43]. Oxygen levels were measured electrochemically using a Cole-Parmer (Vermont Hills, IL) oxymeter fitted with a Clark-type electrode (model 5300; YSI, Yellow Springs, OH) inserted in the same spectrophotometer cuvette; the cuvette was carefully closed with a gas-tight rubber septum to prevent oxygen exchange with the environment and in order to follow mitochondrial oxygen consumption and monitor oxygen levels simultaneously with porphyrin reduction. Control experiments utilizing flavoenzymes such as xanthine oxidase and glucose oxidase which have been previously shown to reduce MnP(III) to MnP(II) [23] were performed in order to validate this set up.

Peroxynitrite-dependent complex I inactivation: antioxidant effect of manganese porphyrins

Complex I–dependent respiration was monitored in SMP through oxygen consumption using a high-resolution respirometer, Oroboros Oxygraph-2k (Oroboros Instruments, Innsbruck, Austria) and by following NADH dehydrogenase activity spectrophotometrically [9]. These experiments were performed at 37°C with 0.1 mg/mL SMP, 1 mM NADH, 5 μM MnP in PBS. For the oxygen consumption studies, after the oxymeter is stabilized, SMP were added followed by NADH. The initial slope of oxygen consumption represents the control respiration for each condition. Once a measurable slope was obtained, a peroxynitrite infusion started at 50 μM/min for 3 minutes by a motor-driven syringe coupled to the oxymeter. When the infusion ended, the chamber was opened for approximately one minute to re-oxygenate the system, restoring an oxygen concentration to *ca.* 100 – 150 μM; then, the oxymeter chamber was closed again, NADH added to avoid substrate depletion and a second slope of oxygen consumption by SMP was obtained (see also the scheme in Fig. 7A). Where indicated, the samples were collected, ultracentrifuged to concentrate them and then separated by electrophoresis and analyzed by western blot immunochemical analysis with anti-3-NO_2 tyrosine and anti-DMPO antibodies. For activity measurements, a similar exposure protocol was used and after peroxynitrite infusion, SMP were diluted to 0.1 mg/mL, additional NADH (200 μM) was added and the reduction of ferricyanide (0.5 mM) in the presence of 5 μM rotenone was followed at 420 nm ($\varepsilon = 1\ mM^{-1}cm^{-1}$) [9].

General Procedures

All experiments reported herein were reproduced at least three times, and results shown correspond to one representative experiment of each one unless otherwise indicated. Graphics and mathematical fits to experimental data were performed using OriginPro 8 (OriginLab Corporation).

RESULTS

Evidence of peroxynitrite formation in submitochondrial particles exposed to •NO

Luminol oxidation produces a chemiluminescence intermediate that allows the detection of peroxynitrite in biological systems with high sensitivity [2]. Indeed, luminol chemiluminescence (LCL) induced by both $O_2^{\bullet-}$ and peroxynitrite was previously assessed by our group [32,33]; it was shown that pure peroxynitrite induces LCL and that LCL induced by $O_2^{\bullet-}$ was inhibited at first by addition of excess •NO by trapping of luminol-derived radicals, followed by a characteristic “overshoot” of light emission corresponding with peroxynitrite-dependent LCL. In this work, we applied LCL to establish the formation of peroxynitrite by SMP.

In figure 1, we evaluated peroxynitrite production by SMP (0.5 mg/mL) exposed to •NO. SMP were incubated with luminol for 5 minutes under continuous shaking at 37°C. Initially,

succinate was added and no light emission was obtained. Then, antimycin A was added and LCL was stimulated. Superoxide radical favors luminol oxidation to an unstable luminol endoperoxide, which decays emitting light [2]. The maximal $O_2^{\bullet-}$ flux from SMP was estimated as 1.9 nmol mg^{-1} min^{-1}, which translates to the range of 1 – 1.4 μM/min in the system under study (0.5 – 0.75 mg/mL). The addition of a bolus of $^{\bullet}NO$ (6 μM) to the suspension showed a transient inhibition of LCL, followed by an overshoot in light emission corresponding to peroxynitrite formation [33] by SMP, that stabilizes at greater values than the initial $O_2^{\bullet-}$-dependent LCL due to enhanced rates of mitochondrial $O_2^{\bullet-}$ formation after peroxynitrite-dependent damage of mitochondrial electron transport components [9][1]. LCL was totally inhibited by the addition of SOD (2 μM), indicating the involvement of $O_2^{\bullet-}$ in the chemiexcitation mechanism (Fig. 1A).

In figure 1B, bars represent the steady-state levels of LCL by SMP exposed to succinate and antimycin A under various conditions. A dose-dependent increase of LCL was obtained when the $^{\bullet}NO$ donor NOC-7 was added up to 3 μM (*i.e.* 0.3 μM/min $^{\bullet}NO$), but at the higher concentration of 6 μM NOC-7 (0.45 μM/min de $^{\bullet}NO$), LCL inhibition was compatible with the preferential fate of luminol-derived species to “dark routes” by excess of $^{\bullet}NO$ [33]. Addition of the peroxynitrite scavenger methionine (k = 200 $M^{-1}s^{-1}$) or SOD also inhibited LCL.

SMP were also capable of inducing coelenterazine chemiluminescence (CCL) (Fig. 2A). Interestingly, the sole addition of succinate to SMP resulted in CCL, evidencing the “basal” levels of $O_2^{\bullet-}$ generation and compatible with a higher sensitivity of the probe in comparison with luminol. Further addition of antimycin A caused a large increase in CCL, as expected from the enhanced $O_2^{\bullet-}$ formation rates by SMP. Similar to what was observed with LCL, bolus addition of $^{\bullet}NO$ resulted on a transient inhibition followed by an “overshoot”, in agreement with our previous report where CCL was induced by xanthine/xanthine oxidase and modulated by $^{\bullet}NO$ levels [35]. The evidence of peroxynitrite formation in SMP exposed to $^{\bullet}NO$ by CCL was further confirmed by the inhibitory effect that pre-incubation with methionine had on CCL emission profile after $^{\bullet}NO$ addition (Fig. 2B). To note, coelenterazine does not react directly with peroxynitrite, but rather with peroxynitrite-derived radicals as revealed by stopped-flow based measurements (Valez *et al*, unpublished data).

In figure 3, peroxynitrite formation was also measured by fluorescence through DHR oxidation to rhodamine–123 (RH). We mixed SMP with DHR in PBS with succinate as substrate, and antimycin A; immediately, NOC-7 was added to the mixture and the fluorescence was followed for 20 minutes. Increasing concentrations of NOC-7 corresponding to up to 1.4 μM min^{-1} $^{\bullet}NO$ produced faster increases in RH fluorescence, reflecting peroxynitrite formation. However, higher fluxes of $^{\bullet}NO$ showed a decrease in RH fluorescence, displaying an overall bell–shaped curve (Fig. 3A). DHR reacts with peroxynitrite-derived radicals ($^{\bullet}NO_2$ and $^{\bullet}OH$), instead of reacting directly with peroxynitrite [44] and therefore the inhibitory action of excess $^{\bullet}NO$ is expected due to its reaction with semi-oxidized DHR radical intermediates [41]. Maximal yields of RH formation were obtained at close to equimolar $^{\bullet}NO$ and $O_2^{\bullet-}$ fluxes. Pre-incubation with methionine results in a strong inhibition of $^{\bullet}NO + O_2^{\bullet-}$-dependent DHR oxidation, supporting the peroxynitrite-mediated process (Fig. 3B).

A novel fluorescent probe for peroxynitrite detection was assessed in SMP. In CBA (coumarin-7-boronic acid), the boronic acid reacts stoichiometrically and fast with $ONOO^-$

[1]With the initial flux of $O_2^{\bullet-}$ and the amount of $^{\bullet}$ NO added, all of the peroxynitrite is formed and decomposed (including reactions with luminol) within the first 1–2 minutes [1].

with a rate constant of 1.1×10^6 M^{-1} s^{-1} yielding the hydroxylated product, 7-hydroxycoumarin (COH), borate and nitrite [19]. In figure 4, succinate, antimycin A and NOC-7 were added into the SMP system resulting in a linear increase over time in fluorescence due to COH accumulation reflecting peroxynitrite formation by the simultaneous fluxes of $^{\bullet}NO$ and $O_2^{\bullet-}$. Unlike DHR which had a bell-shaped response as a function of NOC-7 concentration, CBA showed an increase in the slope of fluorescence that reached a plateau at higher $^{\bullet}NO$ fluxes (Fig. 4A). This behavior is due to the direct reaction of CBA with peroxynitrite [19], involving a direct two-electron oxidation process without significant formation of probe-derived radical intermediates that otherwise could react with $^{\bullet}NO$[2]. Inhibition of the CBA signal was obtained by cysteine ($k = 4.5 \times 10^3$ M^{-1} s^{-1}) at concentrations that compete efficiently for peroxynitrite (Fig. 4B) [29]. Notably, for both the DHR and CBA assays, the maximum of probe oxidation induced by SMP was obtained at *ca.* 25 μM NOC-7, suggesting that under those conditions, the $O_2^{\bullet-}$ and $^{\bullet}NO$ flux ration was close to one.

Peroxynitrite-induced protein oxidation in SMP

Peroxynitrite-derived radicals react with mitochondrial inner membrane proteins leading to the generation of protein radicals that could be trapped with DMPO, which are further oxidized to stable nitrones; the protein-DMPO nitrone products can be immunochemically detected by a specific antibody, in a process overall known as immunospintrapping [45]. In figure 5, SMP were pre-incubated with DMPO (lanes 1–8) and exposed to different reagents for 30 minutes at 37°C. Significant immunodetection in SMP was obtained upon preincubation with succinate, antimycin A and increasing concentrations of NOC-7, compatible with peroxynitrite formation. Addition of SOD or tiron (to scavenge $O_2^{\bullet-}$) or methionine (to scavenge peroxynitrite) inhibited protein radical formation as revealed immunochemically. Protein tyrosine nitration was also detected in the condition of maximal peroxynitrite formation, although the signals were much weaker than for the protein radical detection (not shown). Control conditions showed that neither $O_2^{\bullet-}$ nor $^{\bullet}NO$ fluxes alone resulted in protein radical formation and also pre-incubation with methionine inhibit the immunodetection (Fig. 5B).

Manganese porphyrin reduction and antioxidant capacity in SMP

Previous work in our lab showed that under low oxygen tensions complexes I and II of the mitochondrial electron transport chain can reduce MnP(III) to MnP(II), which can in turn reduce $ONOO^-$ to NO_2^- and protect mitochondrial components from peroxynitrite-mediated injury [23]. Taking into account that inside mitochondria under physiological conditions oxygen concentration is typically in the 3–30 μM range [24], we evaluated whether physiologically–relevant oxygen concentrations are adequate to ensure sufficient MnP reduction, and thus be protective against peroxynitrite-mediated impairments. Oxygen consumption and MnP reduction were monitored simultaneously electrochemically and spectrophotometrically, respectively. In figure 6, MnP (MnTE-2-PyP) reduction was evaluated following the absorbance at 454 and 439 nm corresponding to the maxima of Mn(III) and Mn(II), respectively [43]. For complex I (Fig. 6A), we observed MnP reduction starting at relatively high oxygen concentrations (*e.g.*at 150 μM) and continuing steadily while oxygen was being consumed by SMP plus NADH in the first 4 – 5 minutes; at 10 μM oxygen almost a 100% of the MnP (5 μM) was reduced to Mn(II). In the case of complex II (Fig. 6B), the reduction of MnP by succinate was much slower, taking 20 – 25 minutes to complete the process. Complex II-dependent MnP reduction was significantly accelerated at low oxygen concentrations, < 10 μM. Furthermore, we evaluated another MnP,

[2]The slight decrease of COH yield at higher NOC-7 concentration may be attributed to the reaction of $^{\bullet}NO$ with a minor free radical route (<20 %) during peroxynitrite-dependent CBA oxidation [20].

MnTnHex-2-PyP that has similar reactivity with peroxynitrite [46] as MnTE-2-PyP but a higher reduction potential ($E_{1/2}$ ° = +0.314 V) and contains four alkyl chains with six carbon atoms that increase the lipophilicity [47]. In Fig. 6C, MnTnHex-2-PyP was almost completely reduced by complex I with NADH within the mixing time (1 – 2 min) even though oxygen levels were still very high (>100 μM, data not shown). At 10 μM oxygen, all of the MnTnHex-2-PyP was reduced. Moreover, reduction by complex II with succinate (fig. 6D) showed a similarly fast behavior, being complete in the first 3–4 minutes (at that time the oxygen level was > 100 μM, so at 10 μM the reduction was total). Overall, the results with MnTnHex-2-PyP are consistent with a very rapid reduction process by both complex I and II, in line with its higher reduction potential ($E_{1/2}$ ° = +0.314 V) than that of MnTE-2-PyP ($E_{1/2}$ ° = +0.228 V) (Fig. 6E).

Antioxidant effect of manganese porphyrin in SMP exposed to authentic $ONOO^-$ fluxes

We assessed if MnP reduced by the electron transport chain components could protect mitochondrial complexes against peroxynitrite-mediated damage, particularly in complex I that readily reduces MnP (Fig. 6) and is known to be sensitive to peroxynitrite-mediated inactivation [6,9].

In figure 7, we evaluated complex I dependent-oxygen consumption in SMP with NADH as substrate with or without MnP challenged by a peroxynitrite flux of 50 μM/min; the protocol of addition of reactants was the same as indicated in Fig. 7A. MnP were reduced during the SMP-dependent oxygen consumption process until near-to-anoxic levels were reached; then, peroxynitrite was infused for 3 minutes, followed by reoxygenation. We observed that under control conditions (without MnP and peroxynitrite), SMP respiratory rates after anoxia/reoxygenation decreased by ~25% compared with the pre-anoxic condition. When peroxynitrite was infused for 3 minutes, there was a ~ 65% decrease in respiratory rate. Pre-incubation of SMP with MnP totally prevented the peroxynitrite-mediated effects on complex I, and protected from anoxia/reoxygenation, with only a ~ 7% loss of respiratory rate in the presence of MnP over the pre-anoxic condition (Fig. 7B). In agreement with the complex I oxygen consumption data, peroxynitrite infusion caused ~60 % loss in NADH dehydrogenase activity (control activity = 0.89 μmol min^{-1} mg^{-1}) which was largely protected in the presence of MnP, with only a ~ 20% inactivation (*i.e.* an extent of inactivation that does not impact overall respiratory rates).

We also analyzed the effects of MnP on the formation of protein radicals in SMP by an endogenous flux of peroxynitrite (Fig. 8). Peroxynitrite was generated in SMP with succinate, antimycin A and NOC-7 in 1.5 mL-capped microcentrifuge tubes to minimize oxygen entry and facilitate MnP reduction. Immunospintrapping (as in Fig. 5), showed that the peroxynitrite-dependent protein radical formation was totally inhibited in the presence of MnP. It is estimated that during the incubation period, overall peroxynitrite formation by SMP under maximal conditions was > 20 μM; as total protection was obtained with 5 μM MnP, this is consistent with the catalytic reduction of peroxynitrite.

Another important effect of $ONOO^-$ mediated-damage is nitration of protein tyrosine residues. To further explore the protective effect on MnP on peroxynitrite-dependent mitochondrial damage, immunochemical analyses of tyrosine nitrated proteins were performed in SMP (Fig. 9). SMP were incubated with or without MnP before exposure to a constant flux of authentic peroxynitrite with the experimental design described in Fig. 7A. The data show that both (pre-reduced) MnTE-2-PyP and MnTnHex-2-PyP (5 μM) significantly attenuated tyrosine nitration in SMP exposed to peroxynitrite fluxes (100 μM/min for 3 minutes, total exposure 300 μM), further supporting the antioxidant (catalytic) capacity of MnP over peroxynitrite in this system.

DISCUSION

In this work, we demonstrated the formation of peroxynitrite from $O_2^{\bullet-}$-forming SMP in the presence of an exogenous source of $^{\bullet}NO$ through a combination of methods. Both tested chemiluminescence probes, luminol and coelenterazine, were capable of revealing peroxynitrite formation, with similar overall patterns of chemiluminescence. Secondary to addition of bolus $^{\bullet}NO$ or exposure to a sustained $^{\bullet}NO$ production by NOC-7 to SMP resulted in either an “overshoot” or enhanced steady-state in light emission, respectively (Figs. 1 and 2). The inhibition of luminol and coelenterazine-dependent chemiluminescence by excess $^{\bullet}NO$ disclosed the free radical nature of both chemiexcitation processes, that lead to the intermediate formation of luminol- or coelentarazine-derived radicals which can readily combine with $^{\bullet}NO$ and promote the formation of probe-derived end products *via* dark routes [33,35]. Similar results were obtained with DHR (Fig. 3), as formation of the fluorescence oxidation product RH was significant only when $O_2^{\bullet-}$ and $^{\bullet}NO$ were formed together. DHR oxidation yield by $O_2^{\bullet-}$-producing SMP displayed a bell-shaped curve as a function of $^{\bullet}NO$ because of the competing reaction of DHR radical intermediates with $^{\bullet}NO$. A similar behavior for DHR has been observed previously in other $O_2^{\bullet-}$ and $^{\bullet}NO$-forming systems [44,48] and reflects the radical nature of the probe oxidation process, which certainly limits the precision in the detection of peroxynitrite. In any event, if we consider the peak of RH formation and a *ca.* 30 % oxidation yield by peroxynitrite [2], a maximal flux of 1.4 μM min^{-1} of peroxynitrite can be estimated, in the presence of a $O_2^{\bullet-}$ flux of 1.4 μM min^{-1} from 0.75 mg/mL SMP and a $^{\bullet}NO$ flux of 1.4 μM min^{-1} by NOC-7 (*i.e.* stoichiometric formation of peroxynitrite).

Interestingly, we used the fluorescent probe CBA presented as a promising tool for specific peroxynitrite detection in biological systems [49]. The advantage of this boronate-based probes that reacts rapid and directly with peroxynitrite yielding an oxidation product, COH, than can be easily followed by fluorescence spectroscopy. Again, significant CBA oxidation was mainly obtained under conditions favoring peroxynitrite generation in SMP (*i.e.* supplemented with succinate, antimycin A and NOC-7) (Fig. 4). Notably, the COH-dependent fluorescence increased as function of NOC-7 concentration until reaching a plateau. The small signal obtained by SMP plus succinate and antimycin A in the absence of $^{\bullet}NO$ is due to the slow oxidation of the probe by hydrogen peroxide ($k = 1.5 \pm 0.2$ $M^{-1}s^{-1}$) [19][3]. The boronate-based probes represent one step forward in terms of sensitivity and specificity for peroxynitrite detection in comparison to other widely used ones such as luminol or DHR that react with a large number of one-electron oxidants and participate in secondary reactions (such as reactions with excess $^{\bullet}NO$) that may lead to less quantitative and even confounding data. Taking into consideration a COH reaction yield with peroxynitrite of near 81 %, the quantitated flux of peroxynitrite always reflected stoichiometrically that of the limiting precursor radical, either $^{\bullet}NO$ or $O_2^{\bullet-}$. The result opens the promising possibility to generate mitochondrial-targeted boronates to measure intramitochondrial formation of peroxynitrite.

Peroxynitrite formation by $^{\bullet}NO$-exposed SMP was further substantiated immunochemically by both immunospintrapping and detection of tyrosine nitrated inner mitochondrial proteins. We have previously detected protein-DMPO nitrone adducts in intact mitochondria obtained from the brain and spinal cord of animals undergoing a neurodegenerative condition in which peroxynitrite plays a contributory role. The present data further substantiates that peroxynitrite formation within the mitochondrial environment is capable to secondarily generate protein-derived radicals; in turn, the protein-derived radicals could react with $^{\bullet}NO$

[3]The lack of COH signal under the condition of NOC-7 exposure alone indicates that the low fluxes of $^{\bullet}NO$ used in our work do not lead to significant increases in mitochondrial $O_2^{\bullet-}$ production, although this may be observed at higher $^{\bullet}NO$ exposures [16].

or $^{\bullet}NO_2$ and evolve to 3-nitrotyrosine (although this was, as expected, less sensitive than immunospintrapping as the millimolar DMPO concentrations competed much better for the protein tyrosyl radicals than submicromolar $^{\bullet}NO_2$). Indeed, tyrosine nitrated proteins in mitochondria have been observed in a large number of disease conditions [10] and even under basal conditions [8] and seem to participate in alterations of mitochondrial redox homeostasis. The data presented herein (Fig. 5) show the utility of immunospintrapping to reveal the reaction of peroxynitrite-derived radicals in mitochondria.

Based on published work form our group [23], we also analyzed whether MnP (previously shown to be reduced by substrate supplemented SMP to Mn(II) in the absence of oxygen) can play a role on peroxynitrite removal *via* the following catalytic cycle:

$$\mathrm{Mn(III)P + e^- \xrightarrow{SMP/substrate/ETC} Mn(II)P} \quad (1)$$

$$\mathrm{Mn(II)P + ONOO^- \rightarrow Mn(IV)P + NO_2^-} \quad (2)$$

$$\mathrm{Mn(IV)P + AH \rightarrow Mn(III)P + AH^{\cdot} + H^+} \quad (3)$$

Where AH represents an electron donor such as glutathione, ascorbic acid and uric acid, that can readily react with Mn(IV)P [23].

The first and critical step (reaction 1) requires that the MnP takes up one-electron from the respiratory complexes; this process is in competition with the normal electron transfer towards molecular oxygen. Since lowering the oxygen levels increase the degree of reduction of the respiratory complexes and the likelihood of reaction 1, herein we explored whether MnP could be reduced by the electron transport chain even at normal mitochondrial oxygen levels (*e.g.*3–30 μM) and subsequently reduced the damage caused peroxynitrite. Previous experiments with MnP acting as catalytic reductants in mitochondria were performed under anoxic conditions [23], a situation that is of limited pathophysiological relevance. MnP antioxidant efficacy is related to their ability to accept and donate electrons, and this ability depends on the physicochemical properties of each Mn-based compound. There is a wide variety of MnP differing on hydrophobicity, reduction potential, electric charge, substituents and reactivity among others [47]. MnTE-2-PyP is a hydrophilic metalloporphyrin with $E_{1/2}$ = +0.228 V *vs.* NHE and has been the most commonly used in oxidative stress models. In turn, the novel MnTnHex-2-PyP has a higher redox potential ($E_{1/2}$ = +0.314 V) and longer alkyl chains that enhance lipophylicity. Besides these properties that should influence their redox interactions with the inner mitochondrial membrane, their reactivity with peroxynitrite is similar [47]. Figure 6E shows the redox potential of respiratory complexes I and II, the two MnP used and molecular oxygen. As the redox potential of MnTnHex-2-PyP is slightly greater than that of MnTE-2-PyP, it becomes more suitable to reduction by the respiratory complexes. Indeed, the reduction of MnTE-2-PyP by complex I and II (Fig. 6A and B, respectively) occurs simultaneously with the decrease of oxygen levels during the process. We observed that at 10 μM approximately, MnTE-2-PyP was almost completely reduced by complex I (plus NADH), manifested by an increase of the absorbance at 439 nm. SMP supplemented with succinate, showed a much slower reduction process but at 10 μM oxygen *ca.* 50% of the MnTE-2-PyP was reduced. Furthermore, in the case of MnTnHex-2-PyP reduction the reaction rate is double for complex I and accelerated fivefold for complex II, consistent with their physicochemical characteristics. Then, under conditions of peroxynitrite formation in the SMP system MnTE-2-PyP was capable to largely protect of both peroxynitrite-dependent inactivation of

NADH dehydrogenase activity and inhibition of complex I-dependent oxygen consumption (Fig. 7), supporting the concept that MnP can undergo catalytic redox cycles in mitochondria to protect from peroxynitrite-dependent oxidative damage as proposed in reactions 1–3 and previously [23]. This contention was further confirmed by the protective action of MnP on protein radical (Fig. 8) and nitrotyrosine (Fig. 9) formation. Importantly, the low micromolar levels of MnP (5 μM) that were able to afford protection on much larger (up to 300 μM) concentrations of peroxynitrite are levels achievable in mitochondria *in vivo*, under dose-regimes shown to provide pharmacological action [50].

In conclusion, we have established the formation of peroxynitrite in $O_2^{\bullet -}$ -forming SMP exposed to $^{\bullet}NO$ with a variety of methodologies; in particular, the use of a boronate-based probe (CBA) to quantitate peroxynitrite and immunospintrapping to assess protein oxidative damage further expands the possibilities to measure these processes in intact mitochondria and even in cells. While mitochondrial $O_2^{\bullet -}$ formation in this work was speeded by the use of the respiratory inhibitor antimycin A, the model represents a general example for other conditions that promote electron leakage to molecular oxygen. In addition, we were able to demonstrate that MnP can catalytically reduce peroxynitrite after interacting and taking up electrons from the electron transport chain. On-going work in our laboratory also supports that the observations reported herein in SMP can be recapitulated with intact mitochondria. Thus, our data directly support the formation of peroxynitrite in mitochondria and demonstrate that MnP can undergo a catalytic redox cycle to neutralize peroxynitrite-dependent mitochondrial oxidative damage.

Acknowledgments

VV was partially supported by a fellowship from Agencia Nacional de Investigación e Innovación (ANII), Uruguay. We thank Dr. Joy Joseph (Medical College of Wisconsin) for the synthesis of coumarin-7-boronic acid and Dr. Ronald Mason (National Institutes of Environmental Health Sciences) for supplying the anti-DMPO nitrone antibody. This work was supported by grants from CSIC-Universidad de la República, Uruguay and National Institutes of Health to RR.

References

1. Ferrer-Sueta G, Radi R. Chemical biology of peroxynitrite: kinetics, diffusion, and radicals. ACS Chem Biol. 2009; 4:161–177. [PubMed: 19267456]
2. Radi R, Peluffo G, Alvarez MN, Naviliat M, Cayota A. Unraveling peroxynitrite formation in biological systems. Free Radic Biol Med. 2001; 30:463–488. [PubMed: 11182518]
3. Radi R, Cassina A, Hodara R, Quijano C, Castro L. Peroxynitrite reactions and formation in mitochondria. Free Radic Biol Med. 2002; 33:1451–1464. [PubMed: 12446202]
4. Castro L, Demicheli V, Tortora V, Radi R. Mitochondrial protein tyrosine nitration. Free Radic Res. 2011; 45:37–52. [PubMed: 20942571]
5. Valez, V.; Aicardo, A.; Cassina, A.; Quijano, C.; Radi, R. Oxidative Stress in Mitochondria. In: Pantopoulos, K.; Schipper, H., editors. Principles of Free Radical Biomedicine. Nova Science Publishers, Inc; New York: 2012. p. 283-302.
6. Cassina A, Radi R. Differential inhibitory action of nitric oxide and peroxynitrite on mitochondrial electron transport. Arch Biochem Biophys. 1996; 328:309–316. [PubMed: 8645009]
7. Giulivi C, Poderoso JJ, Boveris A. Production of nitric oxide by mitochondria. J Biol Chem. 1998; 273:11038–11043. [PubMed: 9556586]
8. Sacksteder CA, Qian WJ, Knyushko TV, Wang H, Chin MH, Lacan G, Melega WP, Camp DG 2nd, Smith RD, Smith DJ, Squier TC, Bigelow DJ. Endogenously nitrated proteins in mouse brain: links to neurodegenerative disease. Biochemistry. 2006; 45:8009–8022. [PubMed: 16800626]
9. Radi R, Rodriguez M, Castro L, Telleri R. Inhibition of mitochondrial electron transport by peroxynitrite. Arch Biochem Biophys. 1994; 308:89–95. [PubMed: 8311480]

10. Murray J, Taylor SW, Zhang B, Ghosh SS, Capaldi RA. Oxidative damage to mitochondrial complex I due to peroxynitrite: identification of reactive tyrosines by mass spectrometry. J Biol Chem. 2003; 278:37223–37230. [PubMed: 12857734]
11. Clementi E, Brown GC, Feelisch M, Moncada S. Persistent inhibition of cell respiration by nitric oxide: crucial role of S-nitrosylation of mitochondrial complex I and protective action of glutathione. Proc Natl Acad Sci U S A. 1998; 95:7631–7636. [PubMed: 9636201]
12. Quijano, C.; Cassina, A.; Castro, L.; Rodriguez, M.; Radi, R. T.a.F. Group. Nitric oxide, cell signaling and gene expression. CRC Press; 2006. Peroxynitrite: a mediator of nitric-oxide-dependent mitchondrial dysfunction in pathology; p. 100-142.
13. Kagawa, Y. Proton motive ATP synthesis. Elsevier Science B.V; Amsterdam: 1984.
14. Ghafourifar P, Schenk U, Klein SD, Richter C. Mitochondrial nitric-oxide synthase stimulation causes cytochrome c release from isolated mitochondria. Evidence for intramitochondrial peroxynitrite formation. J Biol Chem. 1999; 274:31185–31188. [PubMed: 10531311]
15. Poderoso JJ, Carreras MC, Lisdero C, Riobo N, Schopfer F, Boveris A. Nitric oxide inhibits electron transfer and increases superoxide radical production in rat heart mitochondria and submitochondrial particles. Arch Biochem Biophys. 1996; 328:85–92. [PubMed: 8638942]
16. Keller JN, Kindy MS, Holtsberg FW, St Clair DK, Yen HC, Germeyer A, Steiner SM, Bruce-Keller AJ, Hutchins JB, Mattson MP. Mitochondrial manganese superoxide dismutase prevents neural apoptosis and reduces ischemic brain injury: suppression of peroxynitrite production, lipid peroxidation, and mitochondrial dysfunction. J Neurosci. 1998; 18:687–697. [PubMed: 9425011]
17. Nin N, Cassina A, Boggia J, Alfonso E, Botti H, Peluffo G, Trostchansky A, Batthyany C, Radi R, Rubbo H, Hurtado FJ. Septic diaphragmatic dysfunction is prevented by Mn(III)porphyrin therapy and inducible nitric oxide synthase inhibition. Intensive Care Med. 2004; 30:2271–2278. [PubMed: 15349724]
18. Wardman P. Fluorescent and luminescent probes for measurement of oxidative and nitrosative species in cells and tissues: progress, pitfalls, and prospects. Free Radic Biol Med. 2007; 43:995–1022. [PubMed: 17761297]
19. Zielonka J, Sikora A, Joseph J, Kalyanaraman B. Peroxynitrite is the major species formed from different flux ratios of co-generated nitric oxide and superoxide: direct reaction with boronate-based fluorescent probe. J Biol Chem. 2010; 285:14210–14216. [PubMed: 20194496]
20. Keszler A, Mason RP, Hogg N. Immuno-spin trapping of hemoglobin and myoglobin radicals derived from nitrite-mediated oxidation. Free Radic Biol Med. 2006; 40:507–515. [PubMed: 16443166]
21. Cassina P, Cassina A, Pehar M, Castellanos R, Gandelman M, de Leon A, Robinson KM, Mason RP, Beckman JS, Barbeito L, Radi R. Mitochondrial dysfunction in SOD1G93A-bearing astrocytes promotes motor neuron degeneration: prevention by mitochondrial-targeted antioxidants. J Neurosci. 2008; 28:4115–4122. [PubMed: 18417691]
22. Ferrer-Sueta G, Batinic-Haberle I, Spasojevic I, Fridovich I, Radi R. Catalytic scavenging of peroxynitrite by isomeric Mn(III) N-methylpyridylporphyrins in the presence of reductants. Chem Res Toxicol. 1999; 12:442–449. [PubMed: 10328755]
23. Ferrer-Sueta G, Hannibal L, Batinic-Haberle I, Radi R. Reduction of manganese porphyrins by flavoenzymes and submitochondrial particles: a catalytic cycle for the reduction of peroxynitrite. Free Radic Biol Med. 2006; 41:503–512. [PubMed: 16843831]
24. Turrens JF. Mitochondrial formation of reactive oxygen species. J Physiol. 2003; 552:335–344. [PubMed: 14561818]
25. Detweiler CD, Deterding LJ, Tomer KB, Chignell CF, Germolec D, Mason RP. Immunological identification of the heart myoglobin radical formed by hydrogen peroxide. Free Radic Biol Med. 2002; 33:364–369. [PubMed: 12126758]
26. Lahaye D, Muthukumaran K, Hung CH, Gryko D, Reboucas JS, Spasojevic I, Batinic-Haberle I, Lindsey JS. Design and synthesis of manganese porphyrins with tailored lipophilicity: investigation of redox properties and superoxide dismutase activity. Bioorg Med Chem. 2007; 15:7066–7086. [PubMed: 17822908]

27. Boveris A, Alvarez S, Bustamante J, Valdez L. Measurement of superoxide radical and hydrogen peroxide production in isolated cells and subcellular organelles. Methods Enzymol. 2002; 349:280–287. [PubMed: 11912917]
28. Ragan, I.; Wilson, MT.; Darley-Usmar, VM.; Lowe, PN. Subfractionation of mitochondria and isolation of the proteins of the oxidative phosphorylation. In: Darley-Usmar, VM.; Rickwood, D.; Wilson, MT., editors. Mitochondria A Practical Approach. IRL Press; Oxford: 1987. p. 79-112.
29. Radi R, Beckman JS, Bush KM, Freeman BA. Peroxynitrite oxidation of sulfhydryls. The cytotoxic potential of superoxide and nitric oxide. J Biol Chem. 1991; 266:4244–4250. [PubMed: 1847917]
30. Bartesaghi S, Valez V, Trujillo M, Peluffo G, Romero N, Zhang H, Kalyanaraman B, Radi R. Mechanistic studies of peroxynitrite-mediated tyrosine nitration in membranes using the hydrophobic probe N-t-BOC-L-tyrosine tert-butyl ester. Biochemistry. 2006; 45:6813–6825. [PubMed: 16734418]
31. Winterbourn CC. Oxidative reactions of hemoglobin. Methods Enzymol. 1990; 186:265–272. [PubMed: 2172706]
32. Radi R, Cosgrove TP, Beckman JS, Freeman BA. Peroxynitrite-induced luminol chemiluminescence. Biochem J. 1993; 290(Pt 1):51–57. [PubMed: 8382481]
33. Castro L, Alvarez MN, Radi R. Modulatory role of nitric oxide on superoxide-dependent luminol chemiluminescence. Arch Biochem Biophys. 1996; 333:179–188. [PubMed: 8806769]
34. Shimomura O, Teranishi K. Light-emitters involved in the luminescence of coelenterazine. Luminescence. 2000; 15:51–58. [PubMed: 10660666]
35. Tarpey MM, White CR, Suarez E, Richardson G, Radi R, Freeman BA. Chemiluminescent detection of oxidants in vascular tissue. Lucigenin but not coelenterazine enhances superoxide formation. Circ Res. 1999; 84:1203–1211. [PubMed: 10347095]
36. Teranishi K, Shimomura O. Coelenterazine analogs as chemiluminescent probe for superoxide anion. Anal Biochem. 1997; 249:37–43. [PubMed: 9193706]
37. Zhou M, Diwu Z, Panchuk-Voloshina N, Haugland RP. A stable nonfluorescent derivative of resorufin for the fluorometric determination of trace hydrogen peroxide: applications in detecting the activity of phagocyte NADPH oxidase and other oxidases. Anal Biochem. 1997; 253:162–168. [PubMed: 9367498]
38. Turrens JF, Alexandre A, Lehninger AL. Ubisemiquinone is the electron donor for superoxide formation by complex III of heart mitochondria. Arch Biochem Biophys. 1985; 237:408–414. [PubMed: 2983613]
39. Radi RA, Rubbo H, Prodanov E. Comparison of the effects of superoxide dismutase and cytochrome c on luminol chemiluminescence produced by xanthine oxidase-catalyzed reactions. Biochim Biophys Acta. 1989; 994:89–93. [PubMed: 2535790]
40. Folkes LK, Patel KB, Wardman P, Wrona M. Kinetics of reaction of nitrogen dioxide with dihydrorhodamine and the reaction of the dihydrorhodamine radical with oxygen: implications for quantifying peroxynitrite formation in cells. Arch Biochem Biophys. 2009; 484:122–126. [PubMed: 18976629]
41. Wrona M, Patel K, Wardman P. Reactivity of 2′,7′-dichlorodihydrofluorescein and dihydrorhodamine 123 and their oxidized forms toward carbonate, nitrogen dioxide, and hydroxyl radicals. Free Radic Biol Med. 2005; 38:262–270. [PubMed: 15607909]
42. Brito C, Naviliat M, Tiscornia AC, Vuillier F, Gualco G, Dighiero G, Radi R, Cayota AM. Peroxynitrite inhibits T lymphocyte activation and proliferation by promoting impairment of tyrosine phosphorylation and peroxynitrite-driven apoptotic death. J Immunol. 1999; 162:3356–3366. [PubMed: 10092790]
43. Ferrer-Sueta G, Quijano C, Alvarez B, Radi R. Reactions of manganese porphyrins and manganese-superoxide dismutase with peroxynitrite. Methods Enzymol. 2002; 349:23–37. [PubMed: 11912912]
44. Miles AM, Bohle DS, Glassbrenner PA, Hansert B, Wink DA, Grisham MB. Modulation of superoxide-dependent oxidation and hydroxylation reactions by nitric oxide. J Biol Chem. 1996; 271:40–47. [PubMed: 8550595]

45. Nakai K, Mason RP. Immunochemical detection of nitric oxide and nitrogen dioxide trapping of the tyrosyl radical and the resulting nitrotyrosine in sperm whale myoglobin. Free Radic Biol Med. 2005; 39:1050–1058. [PubMed: 16198232]

46. Ferrer-Sueta G, Vitturi D, Batinic-Haberle I, Fridovich I, Goldstein S, Czapski G, Radi R. Reactions of manganese porphyrins with peroxynitrite and carbonate radical anion. J Biol Chem. 2003; 278:27432–27438. [PubMed: 12700236]

47. Batinic-Haberle I, Rajic Z, Tovmasyan A, Reboucas JS, Ye X, Leong KW, Dewhirst MW, Vujaskovic Z, Benov L, Spasojevic I. Diverse functions of cationic Mn(III) N-substituted pyridylporphyrins, recognized as SOD mimics. Free Radic Biol Med. 2011; 51:1035–1053. [PubMed: 21616142]

48. Sikora A, Zielonka J, Lopez M, Dybala-Defratyka A, Joseph J, Marcinek A, Kalyanaraman B. Reaction between peroxynitrite and boronates: EPR spin-trapping, HPLC Analyses, and quantum mechanical study of the free radical pathway. Chem Res Toxicol. 2011; 24:687–697. [PubMed: 21434648]

49. Sikora A, Zielonka J, Lopez M, Joseph J, Kalyanaraman B. Direct oxidation of boronates by peroxynitrite: mechanism and implications in fluorescence imaging of peroxynitrite. Free Radic Biol Med. 2009; 47:1401–1407. [PubMed: 19686842]

50. Reboucas JS, Spasojevic I, Batinic-Haberle I. Quality of potent Mn porphyrin-based SOD mimics and peroxynitrite scavengers for pre-clinical mechanistic/therapeutic purposes. J Pharm Biomed Anal. 2008; 48:1046–1049. [PubMed: 18804338]

- Peroxynitrite formation in mitochondria by $^{\bullet}$NO reaction with electron transport chain-derived $O_2^{\bullet-}$
- Boronic acid derivatives as promising probes for mitochondrial peroxynitrite detection
- Immunospintrapping of inner mitochondrial membrane protein radicals secondary to peroxynitrite
- Mn-Porphyrin reduction by the electron transport chain under physiologically-relevant oxygen levels
- Mn(II)Porphyrins reduce mitochondrial peroxynitrite and protect from nitroxidative damage

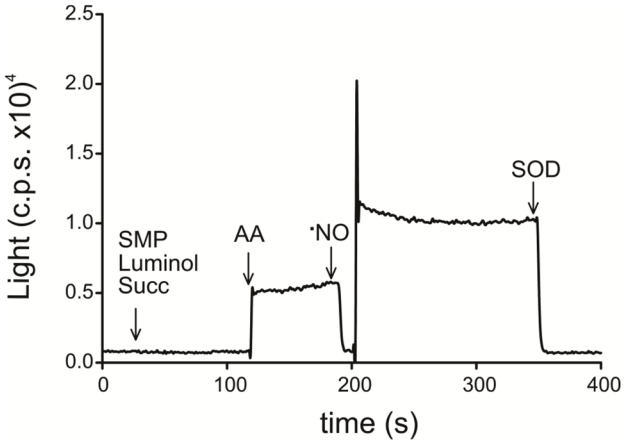

Figure 1A

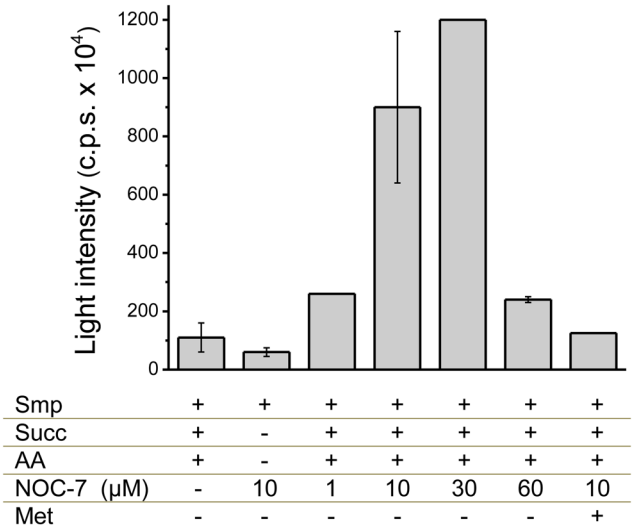

Figure 1B

Fig. 1. Luminol chemiluminescence induced by SMP and the effect of nitric oxide

A) SMP (0.5 mg/mL) were incubated with luminol (400 μM) in isotonic PBS at 37°C. The arrows show the time when (succ, 6 mM), antimycin A (AA, 2 μM), •NO (6 μM), and superoxide dismutase (SOD, 2 μM) were added to the reaction mixture. This experiment was performed in the Thorn Emi photon counter four independent times with similar results; herein we show a representative curve. B) SMP (0.5 mg/mL) were incubated in PBS with 400 μM luminol and different compounds added as indicated: 6 mM succinate, 2 μM antimycin A, and various concentrations of NOC-7; 10 μM methionine (met) was added in the presence of 10 μM NOC-7. Bars represent the maximum chemiluminescence reached in each condition in the LUMIstar Galaxy BMG Labtechnologies.

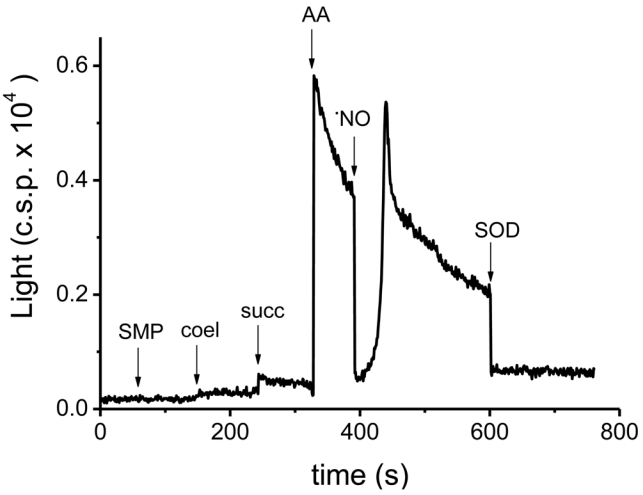

Figure 2A

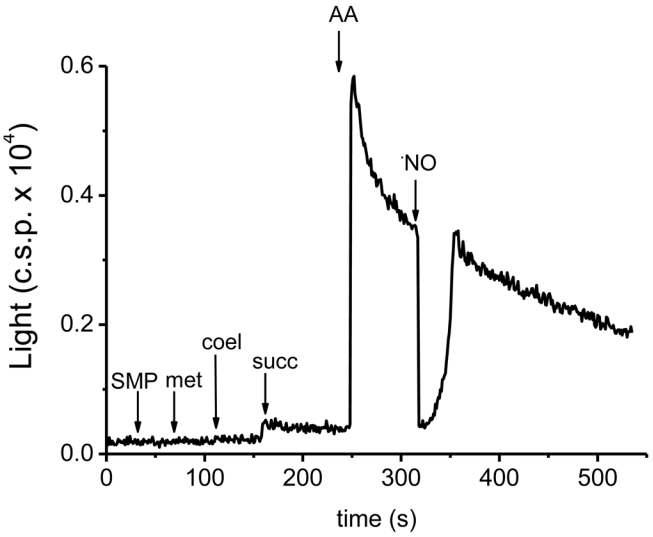

Figure 2B

Fig. 2. Coelenterazine chemiluminescence (CCL) induced by nitric oxide-exposed SMP

A) SMP (0.5 mg/mL) were incubated in PBS with coelenterazine (1 μM) at 37°C. The arrows indicate the order of addition to the reaction mixture of substrate (succ, 6 mM), antimycin A (2μM), the bolus of •NO (6μM) and SOD (2μM). This assay was performed in the same Thorn Emi photon counter used with luminol, four times with similar results. B) We evaluated the pre-incubation of SMP with methionine (5 mM) before the addition of substrates.

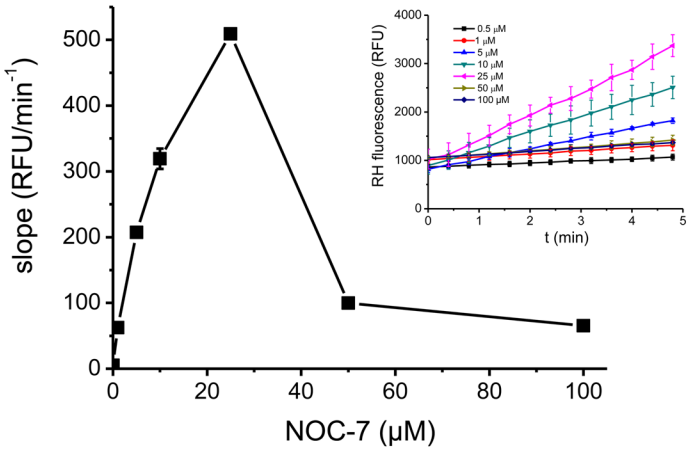

Figure 3A

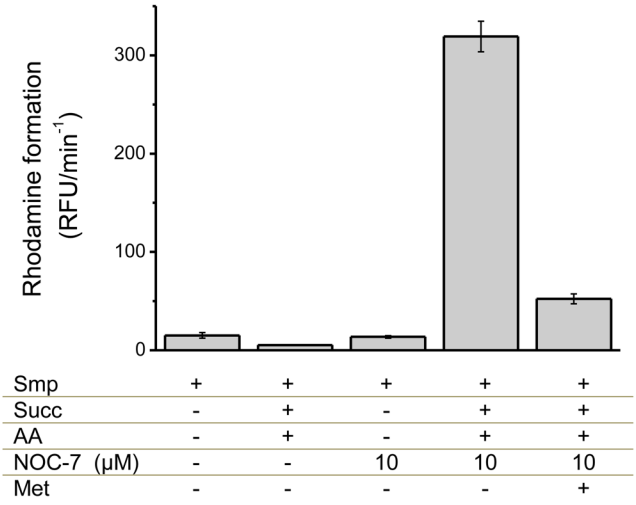

Figure 3B

Fig. 3. Dihydrorhodamine-123 oxidation by nitric oxide-exposed SMP

SMP (0.75 mg/mL) were incubated in PBS with dihydrorhodamine-123 (DHR, 50 μM). Rhodamine-123 fluorescence was followed at 37°C, under continuous agitation for 20 min. A) Fluorescence upon addition of succinate (6 mM), antimycin A (2 μM) as a function of NOC-7 concentrations. *Inset*: time course of RH accumulation B) The effect of methionine (10 mM) in fluorescence yields at 10 μM NOC-7-exposed SMP. Control conditions in the absence of either $O_2^{\bullet -}$ or $^{\bullet}NO$ were performed as indicated.

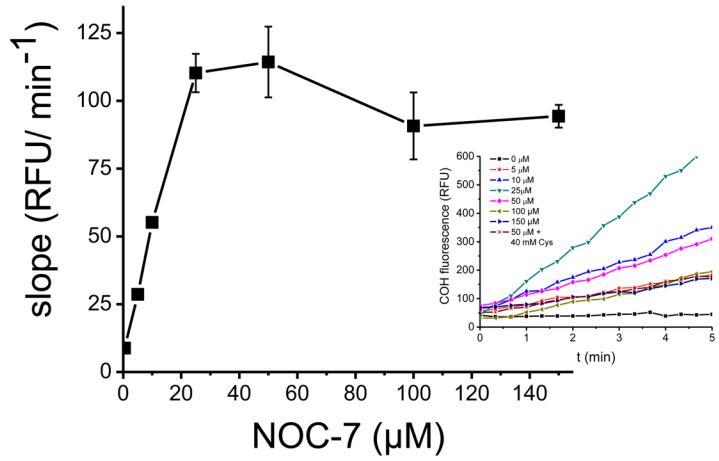

Figure 4A

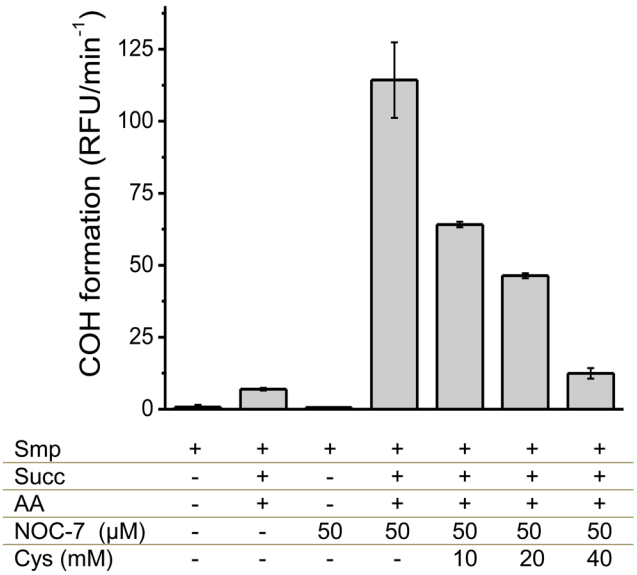

Figure 4B

Fig. 4. Coumarin -7-boronic acid oxidation by SMP

SMP (0.75 mg/mL) were incubated in PBS with coumarin -7-boronic acid (CBA, 50 μM). Fluorescence of the oxidized form, 7-hydroxycoumarin (COH), was followed at 37°C under continuous agitation for 20 min. A) Fluorescence upon addition of succinate (6 mM), antimycin A (2 μM) as a function of NOC-7 concentrations. *Inset*: time course of COH accumulation. B) Controls were performed at 500 μM NOC-7 and the effect of cysteine (20 and 40 mM) on CBA oxidation was tested as well.

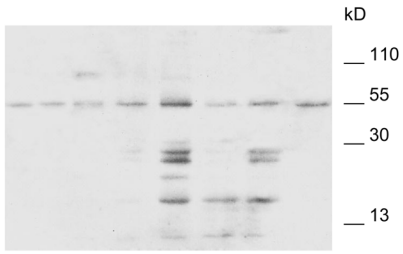

	1	2	3	4	5	6	7	8
Succ	+	-	+	+	+	+	+	+
AA	+	-	+	+	+	+	+	+
NOC-7 (μM)	-	40	10	20	40	40	40	40
SOD	-	-	-	-	-	+	-	-
Met	-	-	-	-	-	-	+	-
Tiron	-	-	-	-	-	-	-	+

Figure 5A

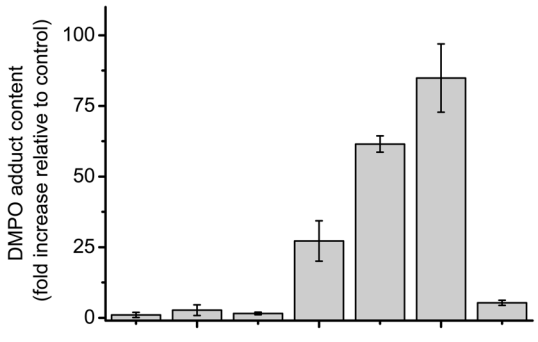

	1	2	3	4	5	6	7
Succ	-	+	-	+	+	+	+
AA	-	+	-	+	+	+	+
NOC-7 (μM)	-	-	25	5	25	50	25
Met	-	-	-	-	-	-	+

Figure 5B

Fig. 5. Detection of protein radical formation in SMP by DMPO immunospintrapping

A) SMP (1 mg/mL) were incubated in isotonic buffer at 37°C for 20 min with DMPO (100 mM) plus different reagents. Succinate (3 mM), antimycin A (2 μM), SOD (20 μM), methionine (10 mM), tiron (5 mM) and NOC-7 (10, 20 and 40 μM) were added as indicated. B) Controls were performed and band densities were represented in bars. Increasing concentrations of NOC-7 (5, 25 and 50 μM) produce augmented immunodetection with anti-DMPO. The inhibitory effect of methionine (10 mM) was tested on protein radical formation.

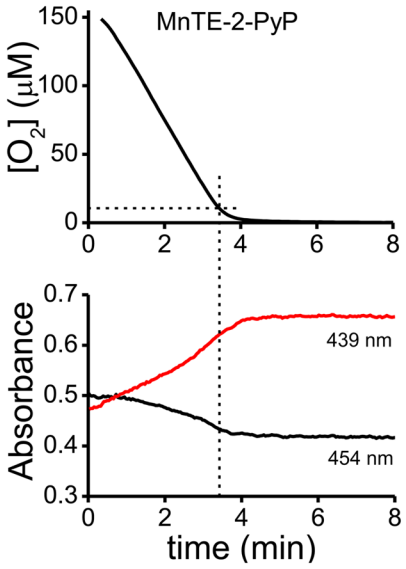

Figure 6A

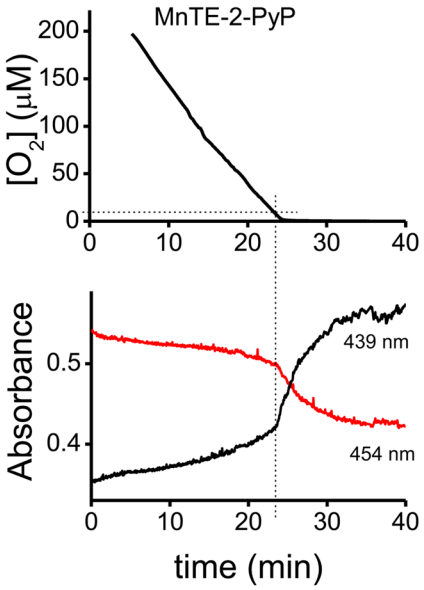

Figure 6B

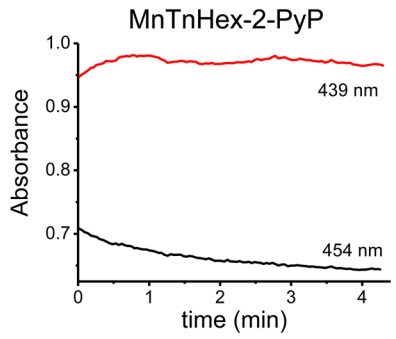

Figure 6C

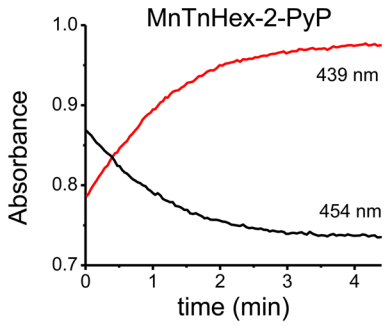

Figure 6D

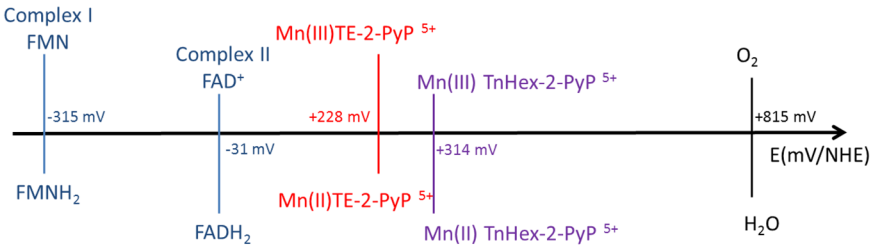

Figure 6E

Fig. 6. MnTE-2-PyP and MnTnHex-2-PyP reduction by SMP as a function of oxygen concentration

Oxygen concentration and MnP reduction were followed simultaneously as indicated under Materials and Methods. A) SMP (0.1 mg/mL) were incubated in isotonic buffer with MnTE-2-PyP (5 μM) and NADH (1 mM) or B) succinate (2.5 mM) for complex I and II-dependent respiration, respectively. C) SMP (0.1 mg/mL) were incubated with MnTnHex-2-PyP (5 μM) and NADH (1 mM) or D) succinate (2.5 mM) for complex I and II, respectively. In the graphs, 10 μM oxygen is indicated with a line to facilitate data analysis. E) Redox potentials scheme of mitochondrial respiratory chain complexes, the MnP used in this work (MnTE-2-PyP and MnTnHex-2-PyP) and molecular oxygen.

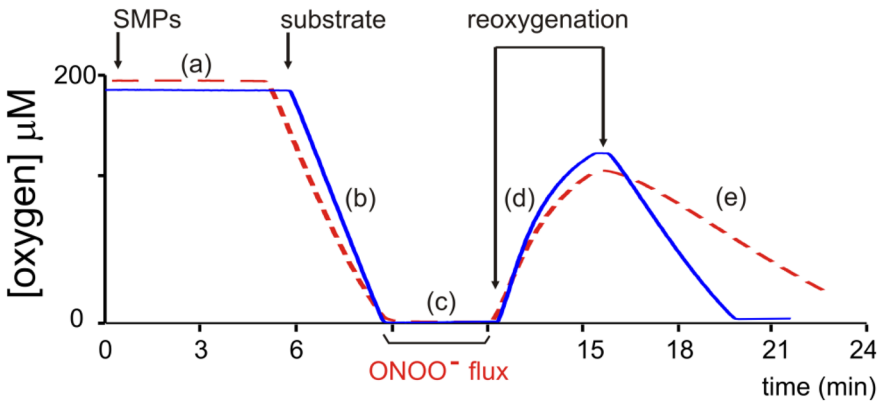

Figure 7A

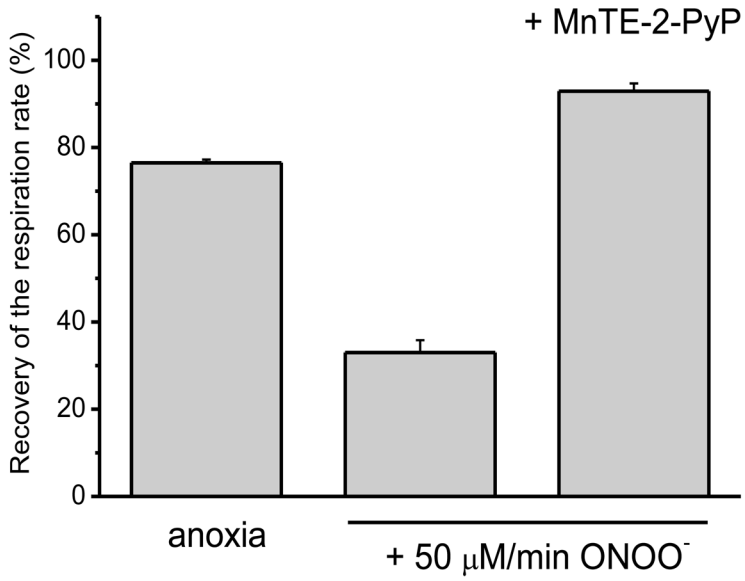

Figure 7B

Fig. 7. Antioxidant effect of MnTE-2-PyP on peroxynitrite-dependent inactivation of mitochondrial complex I

A) Representative primary record of the oxygen concentration as a function of time, evaluating complex I (NADH dehydrogenase)-dependent respiration in SMP before and after a peroxynitrite flux for 3 minutes and the protective capacity of MnP. Once the system is equilibrated and calibrated (a) in PBS at 37 °C with continuous agitation, SMP (0.1 mg/mL) was injected. After that, respiratory substrates were added as indicated and the oxygen consumption starts. This slope (b) corresponds to the 100 % respiratory velocity of each experiment (100%). At near anoxic levels a peroxynitrite flux (50 µM/min) for 3 minutes was initiated (c) and after that the system was reoxygenated by simply opening the chamber

to allow oxygen equilibration (d). When the oxygen level reached *ca.*100 μM, the chamber was closed and substrates were added again leading to a new, post-exposure, slope (e). The solid trace represents a record for SMP plus MnTE-2-PyP added at the beginning of the experiment and the dashed one without MnP just to evaluate the peroxynitrite-mediated inactivation. B) SMP (0.1 mg/mL) were incubated with or without MnTE-2-PyP (5 μM) and NADH (1 mM) is added in isotonic buffer. Bars represent the recovery of the respiratory rate (%) after infusion.

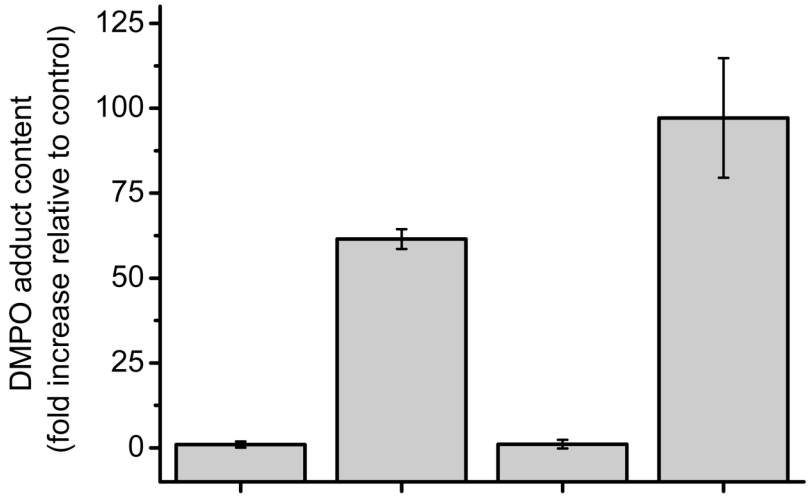

	1	2	3	4
Succ	-	+	+	-
AA	-	+	+	-
NOC-7 (μM)	-	25	25	-
MnTE-2-PyP	-	-	+	-
$ONOO^-$	-	-	-	+

Fig. 8. Mn-Porphyrins protect from peroxynitrite-dependent protein radical formation in SMP

SMP (2 mg/mL) were incubated in capped eppendorf tubes with DMPO (100 mM), succinate (6 mM) and MnTE-2-PyP (5 μM) (when indicated) in isotonic buffer at 37°C with continuous shaking for 5 minutes to allow MnP reduction. After that, NOC-7 (25 μM) were added as indicated for 20 minutes. Samples were ultra-centrifuged to concentrate them to 40 mg/mL and western blot analyses were performed using anti-DMPO antibody. Results were expressed as a function of fold increase relative to control samples.

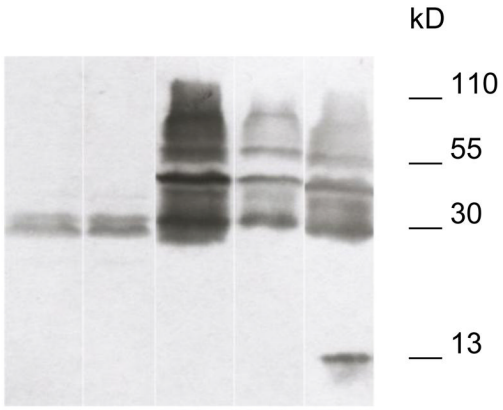

	1	2	3	4	5
SMP/succ	+	+	+	+	+
MnTE-2-PyP	-	+	-	+	-
MnTnHex-2-PyP	-	-	-	-	+
$ONOO^-$	-	-	+	+	+

Fig. 9. Mn-Porphyrins protect from peroxynitrite-dependent protein tyrosine nitration in SMP

Protein tyrosine nitration was assessed in SMP (0.1 mg/mL) incubated with MnTE-2-PyP or MnTnHex-2-PyP (5 μM) and exposed to $ONOO^-$ fluxes (100 μM/min) during 3 minutes in isotonic buffer. Samples were collected and ultra-centrifuged at 100,000 *g*, resuspended to 40 mg/mL, and analyzed by Western blot using anti -nitro tyrosine antibody.